Sigma Journal of Engineering and Natural Sciences
Web page info: https://sigma.yildiz.edu.tr
DOI: 10.14744/sigma.2022.00031

Research Article

The effects of various parameters on the accuracy of kinematic PPP in different platforms

Mert GURTURK[1]*, Metin SOYCAN[1]

[1]*Department of Geomatic Engineering, Yildiz Technical University, Istanbul, Türkiye*

ARTICLE INFO

Article history
Received: 10 September 2020
Accepted: 23 March 2021

Key words:
GNSS; Kinematic PPP; Effective Parameters; Relative Point Positioning

ABSTRACT

The Precise Point Positioning (PPP) technique has become an alternative to relative point positioning techniques in the evaluation of Global Navigation Satellite System (GNSS) data because of its less labor and cost-effectiveness. However, there are many parameters (integer ambiguity resolution, satellite geometry, filter type, atmospheric delays, satellite clock offsets and frequency types) to consider in kinematic PPP and these can have different effects on different platforms. This study, therefore, investigated the effects of various parameters on the accuracy and convergence time of kinematic PPP in different platforms. 3-hour GNSS data, acquired simultaneously from two different receivers (mounted on static and moving platforms), were evaluated using the Kinematic PPP method with different processing parameters in the following four scenarios: satellite combination and geometry, tropospheric model and clock product, all of which have effective roles to play in kinematic PPP processing. The results show that the effect of these parameters in terms of positioning accuracy were, in descending order, strongest for: satellite combination, satellite geometry, troposphere correction, and clock product scenarios. Notably, in the satellite combination scenarios, some parameters have negative effects of up to meter level in the moving receiver compared with the static receiver.

Cite this article as: Mert G, Metin S. The effects of various parameters on the accuracy of kinematic PPP in different platforms. Sigma J Eng Nat Sci 2022;40(2):268–280.

INTRODUCTION

The Kinematic PPP has become an essential alternative method for determining the position of a static or moving receiver. While the success of the traditional relative technique, which uses double-difference simultaneous observations, depends on the distance between the receivers, this is not possible for the kinematic PPP method as this uses zero-difference observations [1]. In this respect, it has clear advantages in many applications in relation to field logistics and costs [2- 5].

***Corresponding author.**
*E-mail address: mgurturk@yildiz.edu.tr, soycan@yildiz.edu.tr

This paper was recommended for publication in revised form by Regional Editor Pravin Katare

The PPP technique is an improved version of the SPP (Single Point Positioning) technique, which is a form of point positioning that cannot remove clock-error using satellites' broadcast ephemeris, ionospheric and tropospheric delays, and other unmodulated errors and deviations that affect observation quality. A chronological examination of studies conducted using the PPP technique shows that, while the first insight was provided by [6], the initial theoretical information was presented by [7]. [8] then built the correction models and main algorithm of PPP using the precise orbit and clock products provided by IGS. Following this, [9] developed their own approach to carrier phase combination independent from the ionosphere and devised an alternative observation model using the combined code and carrier phase measurements. [10] then evaluated IGS stations with the PPP method kinematically and found that the results were less than 10 cm.

However, because a single receiver is used in the kinematic PPP method, there are a number of parameters, namely satellite combination, satellite geometry, troposphere models and frequency type that must be taken into consideration. These parameters can degrade GNSS positioning accuracy for static or moving platforms in kinematic PPP and may cause errors in positioning accuracy up to the level of a few meters [11]. In the relative positioning method, most of them can be eliminated through difference observations conducted between two receivers; however, in PPP they are largely removed by means of various products provided by IGS [8]. For this reason, choosing the most suitable parameter is important as it will increase the effectiveness of the kinematic PPP method as well as improve the evaluation of the results. Since PPP technique does not use differential techniques, there are some difficulties especially in solving integer ambiguity and consequently convergence time. The traditional float PPP needs an initialization time of more than 30 minute to achieve centimeter-level positioning accuracy [12]. Such long initialization time is not acceptable for a wide variety of applications [13]. In order to improve PPP positioning accuracy as well as shorten its convergence time, the ambiguity resolution (AR) has become a new focus of PPP theory research. Compared with traditional PPP, PPP-AR requires an additional "user-side" process to compute satellite phase biases and provide "producer-side" correction [14]. These methods have been developed to safely solve integer ambiguity in PPP so far. That is, the uncalibrated phase delays (UPD) method proposed by [15], the decoupled clock method by [16] and the integer phase clock method by [17]. Also in PPP data processing, the double to triple-frequency measurement process is important to improve convergence time. [18] reached a 23% improvement in triple frequency PPP float solutions compared to dual frequency. But, the question of how triple-frequency measurements impact the initialization of a PPP solution is still a valid problem and requires further investigation.

Previous studies [13, 19-23] were conducted using a variety of IGS products with data from different years and yielded various results in terms of quality. [19] processed the aircraft's 3-hour GNSS data, the coordinates calculated by differential and PPP operations were observed at the level of approximately 0.05 meters. [21] obtained the sub-meter results by processing the GNSS data collected by car and pedestrian with PPP method. By adding different satellite constellation to the GPS system, [13] provided an improvement of 38% in static situations and 31% in kinematic situations. In [20], static and kinematic testings are investigated by using IGS 5 min, 30s and 5s-interval precise satellite clock products in precise point positioning (PPP) solution. Test results show that the sampling rate of IGS satellite clock has very little effect on the static PPP solution. [22] realized GNSS solutions in three environments where satellite visibility was limited. Test results show the impact of obstacles is especially visible in the case of processing short observation sessions. For longer sessions, the influence of observing conditions on the accuracy of the position determination was clearly reduced. [23] adding tropospheric corrections when processing GPS + GLONASS data only improves horizontal positioning by about 2% on East and about 6% on North, but height is improved by about 12% on Up.

The aim of this study is to evaluate GNSS data obtained from two separate platforms, static and kinematic, in four different parameters including satellite combination, satellite geometry, troposphere correction, and clock product and to research the effect of these cases in different platforms on kinematic PPP in terms of precision and convergence time. Some of these parameters require convergence times of approximately two hours. Considering this situation, 3-hours GNSS observations were used. Four different cases include 13 different variations are implemented, which are GPS and GLONASS system, 4 different satellite geometries obtained by changing satellite configuration, Niell, Saastamonien and SBAS tropospheric corrections, 4 different clock corrections with different time intervals obtained from IGS (International GNSS service) and CODE (Center for Orbit Determination in Europe). The effects of 13 different variations in the kinematic and static environment were analyzed by calculating the difference values from the validated reference solution with CSRS PPP online service and relative solution. Moreover, the convergence times of the 13 parameters applied to both platforms for 10 cm accuracy of latitude longitude and height were investigated.

KINEMATIC PPP PROCESSING MODEL

While orbit and clock errors in equations (1) and (2) are removed using products provided by international services, errors such as relativistic error, Sagnac delay, phase wind up, satellite and receiver antenna phase centre offset and variation, the inter-frequency bias and site displacement

effects such as Earth, ocean tide and atmospheric loading are removed through modeling [24],[8,[9]. The measurements can be modelled by

$$R_i = \rho + c(\delta t_{rcv} - \delta t^{sat}) + T_r + a_i(I + K_{21}) + M_i + \varepsilon_i (i = 1,2) \quad (1)$$

$$\phi_i = \rho + c(\delta t_{rcv} - \delta t^{sat}) + T_r + a_i I + b_i + \lambda_{ik} N_i + \lambda_i \text{ш} + m_i + \varepsilon_i \quad (2)$$

In equations (1) and (2), ϕ and ρ express phase and code measurements, respectively; the subscript (i = 1,2) is used to denote the rover and GNSS satellite index. As common to both pseudorange and carrier-phase, there are several error sources, where; δt_{rcv} is the unknown GNSS receiver time error in seconds, δt^{sat} is the GNSS transmitter's clock error in the unit of seconds. Here, c is the speed of light in meters per second, a_i is the conversion factor between the integrated electron density along the ray path, T_r is slant tropospheric delay in meters which is non-dispersive, K_{21} are the receiver and satellite instrumental delays, which are dependent on the code and frequency, I is the phase/pseudorange ionospheric delay in meters. M_i and m_i represent the effect of multipath, also depending on the code type and frequency, ε is noise for phase and code measurements in meters. Within the carrier-phase model (2), there is also unknown integer phase tracking ambiguity denoted by N_i and is taken from units of carrier-phase cycles to meters through multiplication with the GNSS carrier wavelength λ_{ik}, where k = 1,2 and $\lambda_{L1} \approx 19.0$ cm and $\lambda_{L2} \approx 24.4$ cm for the GNSS, λ_i ш, represents wind-up due to the circular polarization of the electromagnetic signal [25], [26].

In (1) and (2), the geometric range between the user's receiver antenna phase center ($x_{rcv}, y_{rcv}, z_{rcv}$) and the satellite's ($x^{sat}, y^{sat}, z^{sat}$) transmitter antenna phase center is denoted as R^{sat}_{rcv} and given by the following equation (3);

$$R^{sat}_{rcv} = \sqrt{(x^{sat} - x_{rcv})^2 + (y^{sat} - y_{rcv})^2 + (z^{sat} - z_{rcv})^2} \quad (3)$$

Dual-frequency geodetic GNSS receivers are generally used in precise measurement studies. To eliminate the ionosphere effect in the GNSS signal measurements, a linear combination (LC) of dual-frequency measurements is often utilized in GNSS data processing [9], [27], [28] and given by (4) and (5), for pseudorange and carrier-phase observations, respectively;

$$R_{iono-free} = R_1 \left[\frac{f_1^2}{f_1^2 - f_2^2} \right] - R_2 \left[\frac{f_2^2}{f_1^2 - f_2^2} \right] \quad (4)$$

$$\phi_{iono-free} = \phi_1 \left[\frac{f_1^2}{f_1^2 - f_2^2} \right] - \phi_2 \left[\frac{f_2^2}{f_1^2 - f_2^2} \right] \quad (5)$$

Ionosphere-free combination observables are used in PPP to eliminate the first-order (up to 99.9%) ionospheric delays in the pseudorange and carrier phase measurements. However, the ionosphere free combination helps reduce the convergence time in PPP. [29] modeled the second-order ionospheric delay for PPP to accelerate the convergence. It was shown that accounting for the second-order ionospheric delay reduced convergence time of PPP by 15%.

The effect of the troposphere delays in equations (1) and (2) are estimated by GNSS observations based on various (Niell, Saastamoinen and Hopfield) troposphere delays and mapped into zenith direction [26]. The troposphere delay is calculated through the integration along the signal path and mapped the zenith direction using mapping functions. In this study, the following mapping function was used to model tropospheric delays including azimuthal asymmetric components (see, equation (6)). The mapping function in terms of the elevation angle (ELV) and the azimuth angle (A) between the satellite and the receiver was calculated using the following equation:

$$M(ELV) + M_W(ELV)\{1 + \cot(ELV)((G_N \cos(A) + G_E \sin(A))\} \quad (6)$$

Moreover the tropospheric delay can be calculated from equation (7);

$$T_{r,z} = M_h(ELV)Z_h + M(ELV)(Z_T - Z_H) \quad (7)$$

Where;

Z_T : tropospheric zenith total delay (m)
Z_h : tropospheric zenith hydrostatic delay (m)
M_h(ELV) : hydrostatic mapping function
M_w : wet mapping function

The parameter computed from equation (7) was estimated from the Extended Kalman Filter together with the north component of the tropospheric gradient (GN) and the east component of the tropospheric gradient (GE) [30]. ZH is the tropospheric zenith hydrostatic delay in meters, which is calculated using a tropospheric model (either the Saastamoinen, Hopfield, or modified Hopfield model), with the zenith angle z = 0 and relative humidity hrel = 0. Mh (ELV) and Mw (ELV) are the hydrostatic and wet mapping functions, respectively. In this study, the Niell Mapping Function (NMF) was used in both cases.

Precise Ephemerides and Clocks Interpolation

RTKLIB uses the fixed degree (n = 10) polynomial interpolation by Newton-Neville,s. In spite of the precise ephemeris high-order polynomial interpolation, a simple linear interpolation is implemented for precise clocks provided as SP3 or clock RINEX files as:

$$dT^s(t) = \frac{(t_{i+1} - t)dT^s(t_i) + (t - t_i)dT^s(t_{i+1})}{t_{i+1} - t_i} \quad (t_i \le t \le t_{i+1}) \quad (8)$$

For the precise clocks provided by IGS (International GNSS service), the relativistic effect should be corrected as:

$$dT^s(t) = \frac{(t_{i+1}-t)dT^s(t_i)+(t-t_i)dT^s(t_{i+1})}{t_{i+1}-t_i} - 2\frac{r^s(t)^T v^s(t)}{c^2} \quad (8)$$

where, $r^s(t)$ and $v^s(t)$ are the satellite position and velocity derived from the precise ephemerides. For details, refer RTKLIB ver. 2.4.2 Manual [31].

TEST AREA, DATA AND PROCESSING PARAMETERS

The experimental study involved both static and kinematic cases. The data were collected by GNSS receivers mounted on static and moving platforms in the test site of Yildiz Technical University Campus on (DoY: 137) in 2018. The test environment is shown in Figure 1. Figure 1b shows the moving receiver that circled around the athletics track and Figure 1c shows the setup of the static receiver located on the roof of the building (green wildcard). Three-hour (start time: 09.00 UTC, end time: 12.00 UTC) GNSS (GPS+GLONASS) observations for the platforms were gathered under the same conditions using a TOPCON Hiper Pro GNSS receiver. The data were analyzed using the PPP approach to observe the effect of significant parameters in the PPP method on different platforms. Thirteen different variations in total were formed for 4 different cases to determine the effect of evaluation parameters on the precision of kinematic PPP. In this study, the position filter was considered to be converged when the positioning errors reached ±0.1 m and remained within that range.

Because the effect of satellite geometry and combination on PPP was studied, and to prevent observation signals from exposure to different atmospheric error sources, the first and second applications were carried out simultaneously on the same field at a sampling interval of 10 seconds. Additionally, a multipath effect with the suitable satellite view was minimized as both applications were carried out in open sky view.

A reference solution common to both platforms was determined to observe the effect of parameters applied on moving and static receivers. The reference solution was evaluated using the kinematic PPP method with RTKLIB software. The parameters used for this reference solution were those suggested in the literature [32-35]. In the

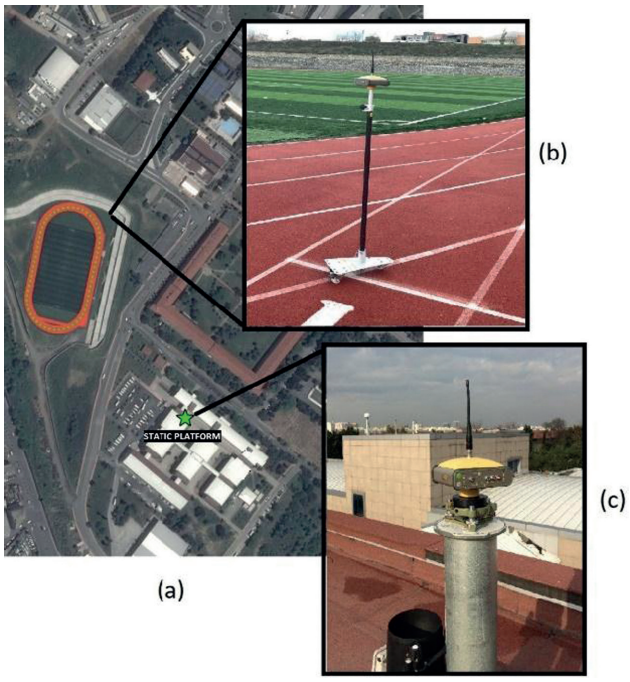

Figure 1: (a) test environment, (b) kinematic field site, (c) static field site.

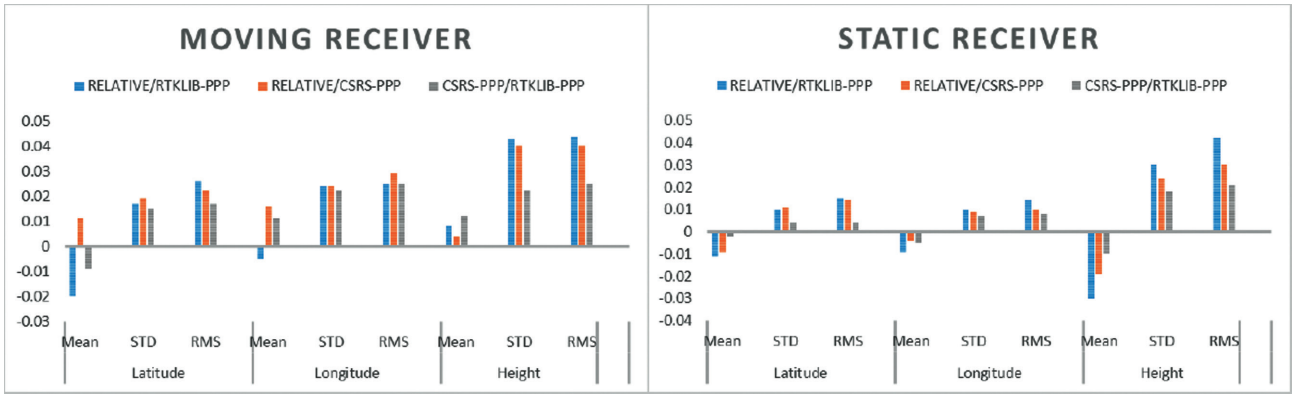

Figure 2. Statistical results obtained by comparing the reference solution with the solutions provided by applying alternative solution techniques. All units are meter.

processing strategy, the ionosphere free linear combination was used, the cut-off angle was 10°, the troposphere was modeled using the NIELL ZTD+Grad model, and a residual wet zenith delay was estimated. Solid Earth tides and ocean loading tides were then modeled, phase windup was considered, and the Kalman estimator was configured for both forward filtering and backwards smoothing.

To test the accuracy of the reference solution, alternative relative and PPP solutions were conducted and compared to the reference solution. The relative solution was conducted using a permanent station, namely YLDZ located approximately 500 meters away from the study field, which was in the EUREF network. For the alternative reference PPP solution, the CSRS-PPP online service was used [36].

Comparative Root Mean Squares (RMS) values obtained from RTKLIB software (reference solution), both with a CSRS-PPP online service and Relative solution, are shown in Figure 2. There is a clear 1-2 cm RMS difference between RTKLIB and CSRS-PPP solutions, and a 1-2 cm RMS difference horizontally and 4 cm RMS difference vertically between RTKLIB and the relative solution. It is clear from these results that the solutions obtained from RTKLIB software are acceptable as a reference solution.

Parameters effective in 4 different kinematic PPP scenarios (13 parameters that are used on both data sets, that is, clock products, troposphere corrections, satellite combinations, satellite geometry) were used in this study (Table 1). RTKLIB version 2.4.2 open-source software was used for PPP applications. RTKLIB is including the applications designed for real-time navigation and post-process positioning. RTKLIB software is based on the user definition of process parameters [37].

An option regarding the solution of PPP-AR (ambiguity resolution) also exists in the RTKLIB software. PPP-AR improves not only the convergence time in kinematic PPP studies, but also the stabilization of the solution. But the most important factor in the kinematic PPP is fixing the integer. Otherwise, the results can be found in meters. For this reason, the ambiguity float solution was conducted in all processes.

The differences between the coordinate values obtained based on 13 parameters and the coordinate values obtained from the reference solution were used to examine the effect of parameters.

ANALYSIS OF RESULTS

The first parameter is the satellite system and the variations of GPS-only, GLONASS-only, and GPS+GLONASS are discussed (Figure 3).

The primary factor that affects convergence time and precision in kinematic PPP applications is the combination of satellite systems. It is clear that multi-constellation approach to PPP method contributes to position precision and convergence time at the rate of up to 25% depending on the increase in the number of satellites [27].The examination of the solution results with GPS-only based on the results of reference solution shows that it carries RMS values of 2-3 cm on kinematic receiver and 1-2 cm on static receiver. The examination of the solution results with GLONASS-only based on the latitude, longitude, and height components shows that they are 11 cm, 9 cm, and 15 cm in the moving receiver and 6 cm, 4 cm, and 10 cm in the static receiver, respectively. Figure 4 shows the RMS values for the differences obtained by subtracting the

Scenarios	Satellite System	Satellite Geometry	Troposphere Correction	Clock Product/Interval
Reference Solution	GPS+GLONASS	Ideal	Niell Ztd+Grad	ESA_CLK_30 Seconds
1	**GPS**	Ideal	Niell Ztd+Grad	ESA_CLK_30 Seconds
	GLONASS	Ideal	Niell Ztd+Grad	ESA_CLK_30 Seconds
2	GPS+GLONASS	**Partially Blocked**	Niell Ztd+Grad	ESA_CLK_30 seconds
	GPS+GLONASS	**Half Blocked**	Niell Ztd+Grad	ESA_CLK_30 seconds
	GPS+GLONASS	**Cut-Off Elevation (30^0)**	Niell Ztd+Grad	ESA_CLK_30 seconds
	GPS+GLONASS	**Least Satellite**	Niell Ztd+Grad	ESA_CLK_30 seconds
3	GPS+GLONASS	Ideal	**Niell Ztd**	ESA_CLK_30 seconds
	GPS+GLONASS	Ideal	**Saastamonien**	ESA_CLK_30 seconds
	GPS+GLONASS	Ideal	**SBAS**	ESA_CLK_30 seconds
4	GPS+GLONASS	Ideal	Niell Ztd+Grad	**IGS_CLK_5 minutes**
	GPS+GLONASS	Ideal	Niell Ztd+Grad	**IGS_CLK_30 seconds**
	GPS+GLONASS	Ideal	Niell Ztd+Grad	**CODE_CLK_30 seconds**
	GPS+GLONASS	Ideal	Niell Ztd+Grad	**CODE_CLK_5 seconds**

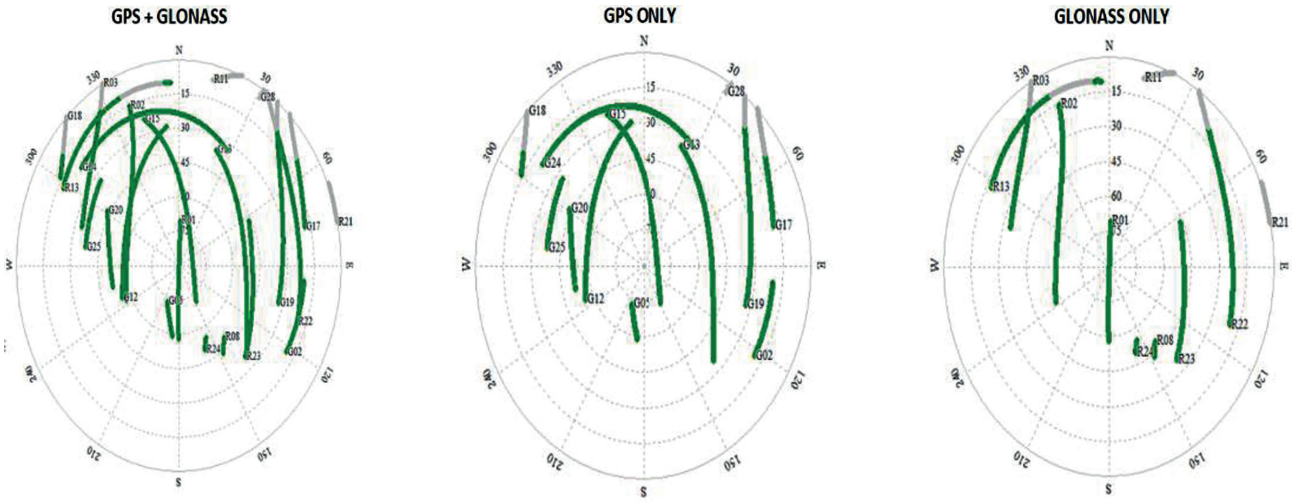

Figure 3. Satellite constellation.

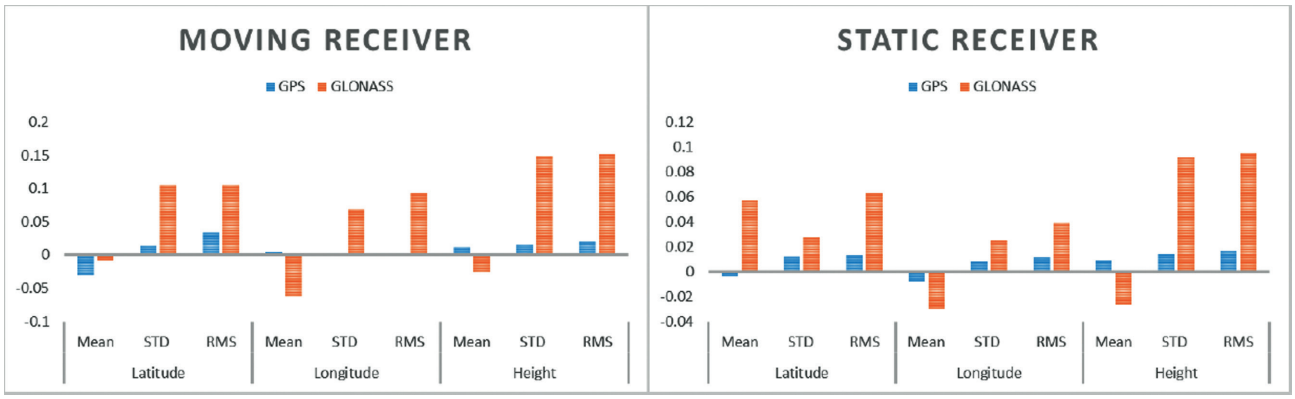

Figure 4. Statistical values of moving receiver and static receiver solutions obtained by applying different satellite combinations to reference solutions. All units are meter.

results from the reference solution under the altered satellite constellation.

Figure 5 shows the convergence time of the satellite constellation parameters of the moving platforms according to the latitude, longitude, height components. GPS-only converges to 10 cm for latitude and height components in 10 minutes and for longitude component in 60 minutes. Convergence was not observed in all components during the observation periods in the GLONASS-only solution. GLONASS-only solution converges to 10 cm accuracy in 40 minutes for latitude and longitude components and in 50 minutes for height component on both platforms except the moving platform. GLONASS-only solution did not converge to the accuracy specified during the measurement in the longitude component of the moving platform, it was observed that GLONASS-only solution was not sufficient for longitude and the GLONASS-only solution required longer observation time.

The second parameter was satellite geometry and 4 different data sets, partially blocked (PB, the number of satellites: 9-11), half blocked (HF, the number of satellites: 8-10), and the least blocked (LS, the number of satellites: 7-6), were formed by creating artificial limitations to prevent satellite geometry on RINEX data, as shown in Figure 6. In addition to these data sets, a new dataset based on the elevation angle was formed by increasing the elevation angle (EL, 30°). This angle was calculated to be equal to the number of satellites observed in the procedure step in which HF was applied.

The comparative results of the different satellite-view data according to the reference solution are given in Figure 7. According to the process results obtained using the Partially Blocked parameter, RMS differences for the components of latitude, longitude, and height were 5 cm, 3 cm, and 8 cm, respectively for the moving receiver and 2 cm, 1 cm, and 4 cm, respectively for the static receiver.

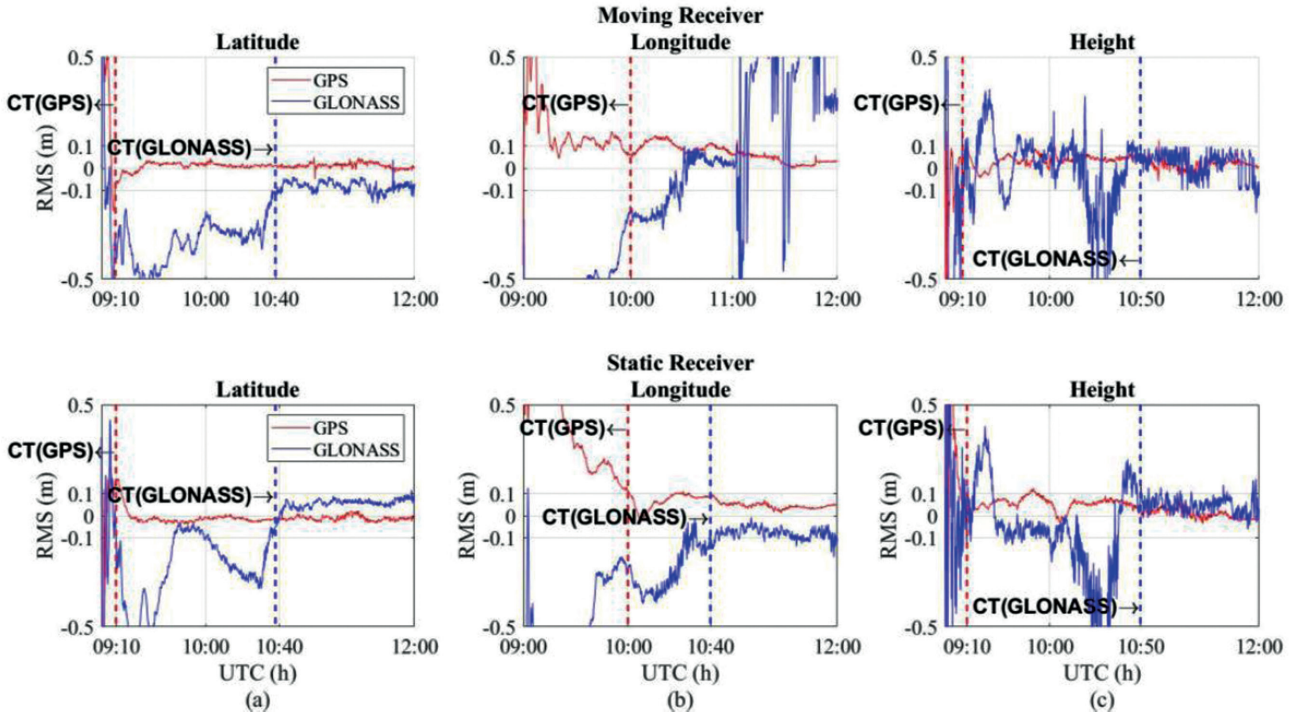

Figure 5. Moving and static receiver results with different satellite combinations (CT: convergence time).

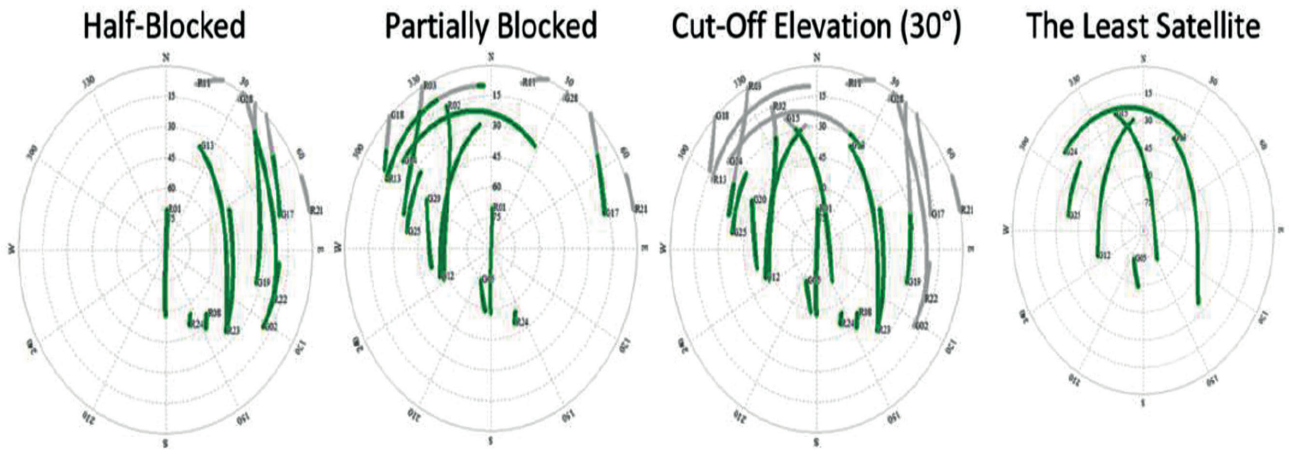

Figure 6. Variations on the satellite geometry.

According to the processing results obtained using the Half Blocked, RMS differences for the components of latitude, longitude, and height were 7 cm, 17 cm, and 6 cm, respectively for the moving receiver and 2 cm, 6 cm, and 4 cm, respectively for the static receiver. According to the processing results obtained using the Cut-0ff Elevation (30°), RMS differences for the components of latitude, longitude, and height were 2 cm, 12 cm, and 5 cm, respectively for the moving receiver and 2 cm, 5 cm, and 4 cm, respectively for the static receiver.

Figure 8 shows the convergence time of the satellite geometry configuration parameters of the platforms according to latitude, longitude and height components. The Partially Blocked parameter converged to 10 cm accuracy in 10 minutes at latitude component, 20 minutes at longitude component and 5 minutes at height component on both parameters. The Cut-0ff Elevation (30°) parameter converged to 10 cm in 25, 20, 25 minutes at latitude, longitude and height components on the static platform, respectively. It converged in 35, 40, 35 minutes on the

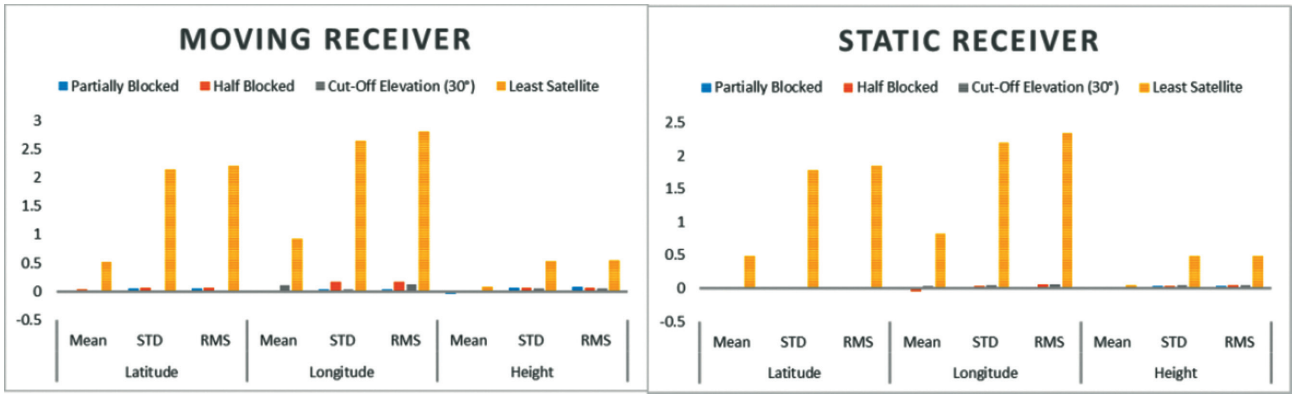

Figure 7. Statistical values of moving receiver and static receiver solutions obtained by applying different satellite geometries to reference solutions All units are meter.

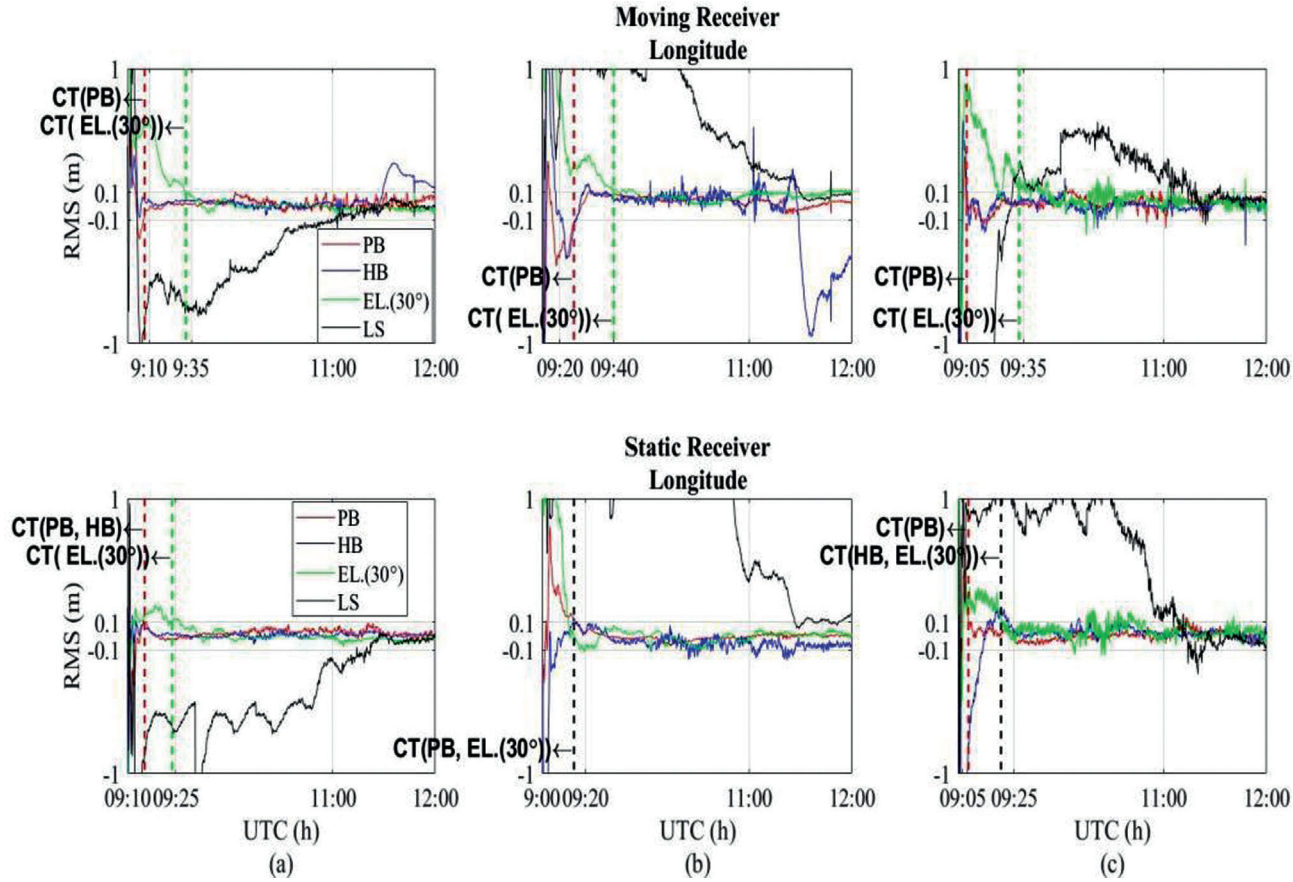

Figure 8. Moving and static receiver results with different satellite geometry (CT: convergence time).

moving platform. The half block parameter converged to 10 cm accuracy in 5, 20, 25 minutes at latitude, longitude and height components on the static platform, respectively. The Least Satellite parameter did not converge to 10 cm accuracy on both platforms during the observation period.

Because the signals that are sent from the satellites are subjected to distorting effects while passing through the atmospheric layers, it is not possible to produce coordinates from these signals directly. The layer that causes the most errors is the troposphere. Although this error source can be eliminated with relative positioning, kinematic PPP requires

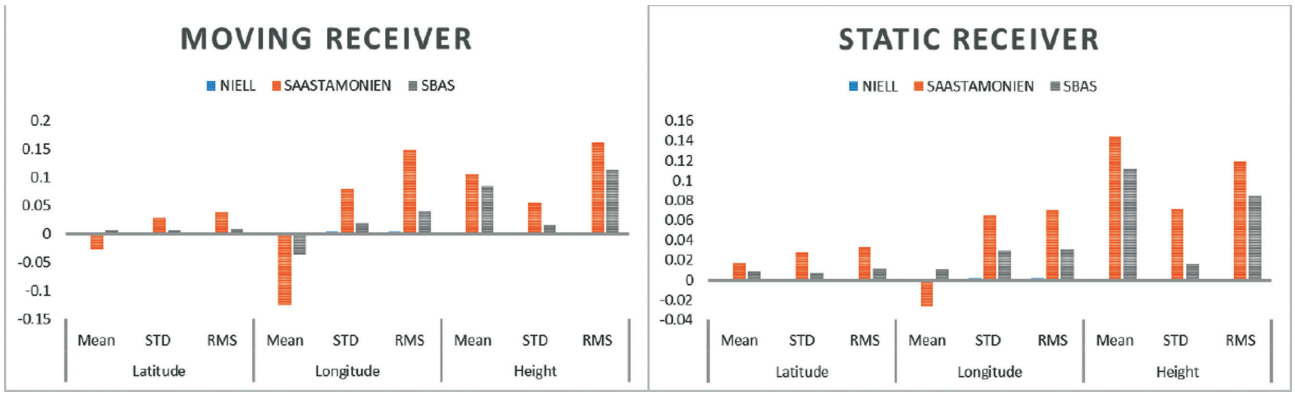

Figure 9. Statistical values of moving receiver and static receiver solutions obtained by applying different tropospheric models to reference solutions. All units are meter.

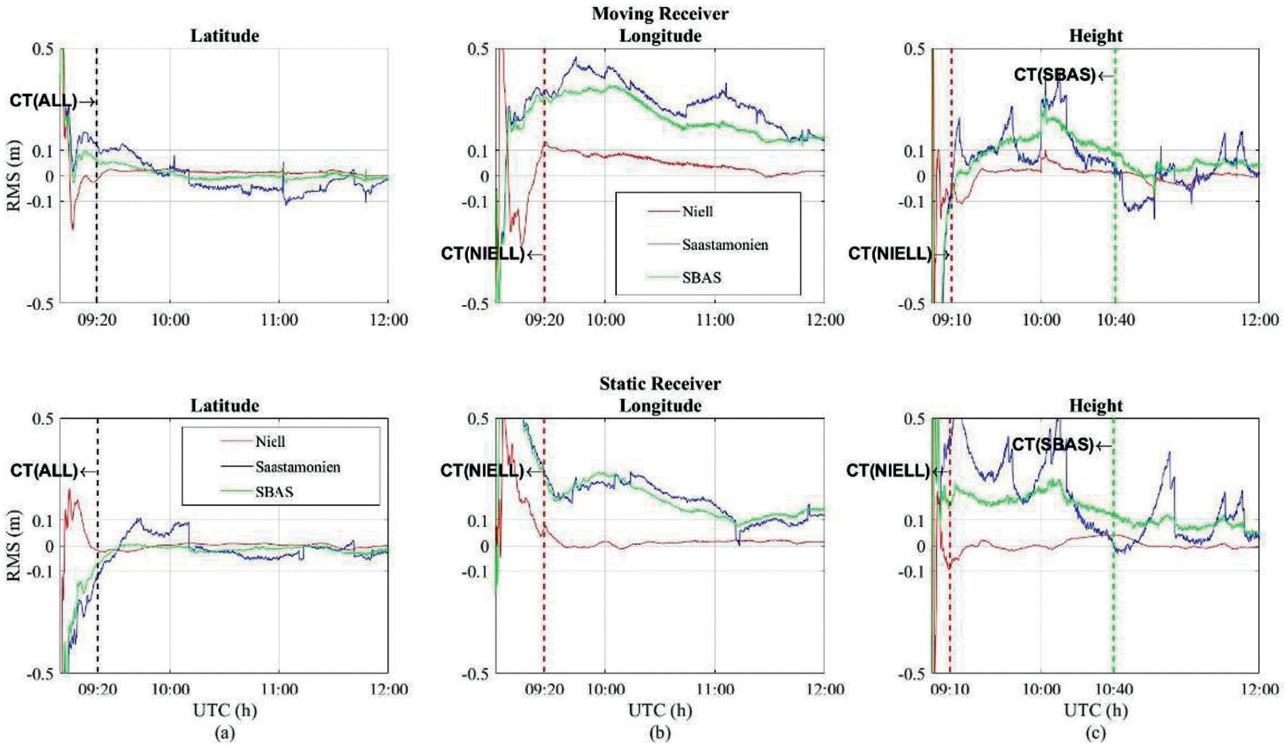

Figure 10. Moving and static receivers results with different tropospheric models (CT: convergence time).

modelling to do so.The troposphere parameters calculated by the Niell, Saastamoinen and RTCA-MOPS (SBAS) model and ZTD values estimated based on GNSS observations. In the 3rd scenario, the effect of the Saastamoinen model [38], Niell troposphere delay model without horizontal gradients [39] and RTCA-MOPS empirical troposphere delay model [40] on kinematic PPP were evaluated. RMS values for the applications in the 3rd scenario are given in Figure 9. Because the field of study for the application in which the Niell troposphere delay model without horizontal gradients is located in the temperate zone latitude, the gradient effect does not significantly affect the results on both moving and static receivers [41].According to the processing results obtained using the Saastamonien model, RMS differences for the components of latitude, longitude, and height were 4 cm, 15 cm, and 12 cm, respectively for the moving receiver and 3 cm, 7 cm, and 16 cm, respectively for the static receiver. According to the processing results obtained using the SBAS tropospheric model, RMS differences for the components of latitude, longitude, and height were 1 cm, 4 cm,

and 11 cm, respectively for the moving receiver and 1 cm, 3 cm, and 9 cm, respectively for the static receiver. These results show that GNSS data gathered from the moving receiver are further affected by tropospheric model change and that the SBAS model is superior to the Saastamonien tropospheric model in both platforms. Figure 10 shows the convergence time of the troposphere model parameters of both platforms according to latitude, longitude and height components. All tropospheric corrections converged in the Latitude component within 20 minutes. It is clear that only Niell solution converges to the specified accuracy in 20 minutes in the longitude component. There are periodic fluctuations in the height component in all three models. Although this situation is relatively eliminated in the SBAS model and mostly removed in the Niell model and the convergence time significantly reduces.

Satellite clock error, which is eliminated through difference observations in the relative evaluation method, is removed using clock products provided by IGS in the PPP method. Based on the calculation between satellite time and GPS time, a deviation of 1 μ leads to an error of 300 m. The sampling interval of the product is significant in removing this error source which must be taken into consideration, especially in kinematic positioning. The more frequent the

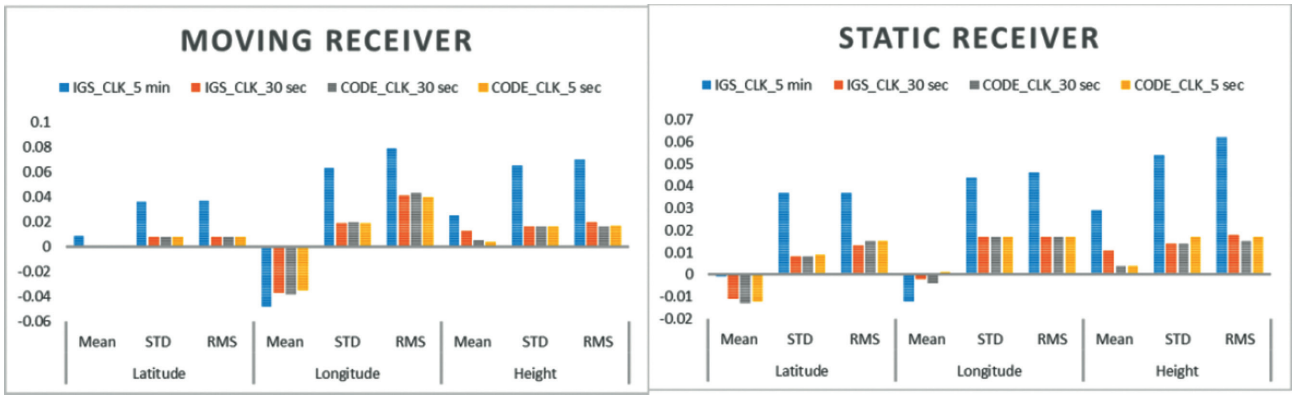

Figure 11. Statistical values of moving receiver and static receiver solutions obtained by applying different clock products to reference solutions all units are meter.

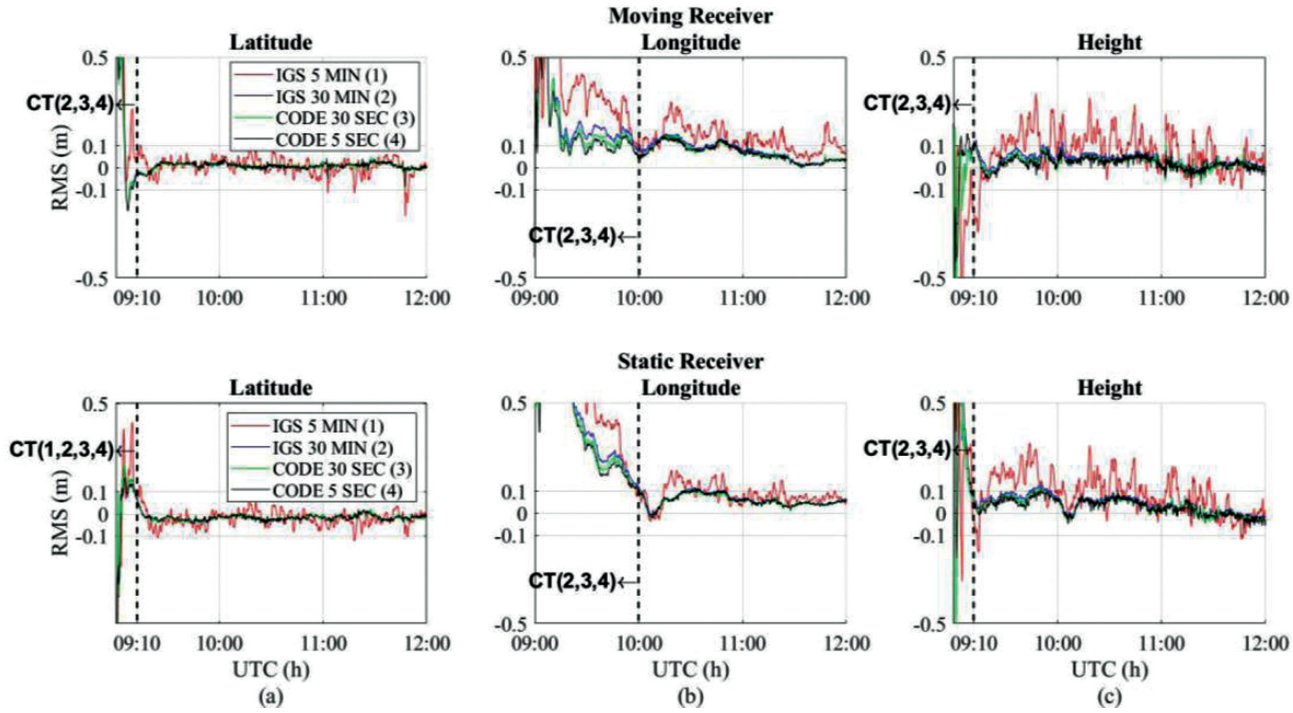

Figure 12. Moving and static platforms results with different clock products (CT: convergence time).

sampling interval of the clock product, the more precise its positioning [10].Clock data variations do not use simple mathematical equations such as orbital data and they are frequently very complex; the satellite clock errors caused by the interpolation are more effective on the positioning accuracy and convergence [42].Therefore, kinematic PPP evaluation was carried out using clock products with different intervals (5 minute, 30 second and 5 second) obtained from a single analysis center such as IGS and CODE (Center for Orbit Determination in Europe) in this step of the scenario. The RMS results obtained are given in Figure 11. Examination of the RMS results obtained using clock products offered by IGS with an interval of 30 seconds and by CODE with intervals of 5 seconds and 30 seconds shows that similar results, with a change of 1-3 mm between 3 different clock products, were obtained. 30 seconds sampling rate clock is dense enough to satisfy the PPP solution [20]. In addition, the results of 5 minutes-clock products offered by IGS were 4 cm, 8 cm, and 7 cm for the components of latitude, longitude, and height, respectively on the moving receiver; and 4 cm, 5 cm, and 6 cm for the components of latitude, longitude, and height, respectively on the static receiver. Examination of the results obtained from both receivers based on clock-product structure shows the significance of clock product intervals in kinematic studies. Figure 12 show the convergence times of clock products parameters on both platforms according to latitude, longitude and height components. In the latitude, longitude and height components, all parameters converged to 10 cm accuracy, except IGS, 5 min at 10, 60, and 10 minutes, respectively.

CONCLUSION

Real-time PPP implementations are currently conducted with the help of a satellite orbit and clock products provided by institutions such as IGS, BKG, CNES, and ESA. However, these implementations cannot provide the expected positioning accuracy in applications conducted by systems such as UAV and GEOTAGGING. For this reason, Post-Process techniques remain a top priority in kinematic PPP. However, there are effective parameters based on user definition that should be taken into consideration for Post-Process kinematic PPP implementations.

In this study, GNSS data was collected from a static and a moving receiver to observe the influence of the aforementioned parameters in the positioning of different platforms. Thirteen different parameters were formed for 4 different scenarios and the effect of evaluation parameters on the precision of kinematic PPP was investigated. The analysis of 4 cases applied to different platforms and the results of 13 different solutions derived from these revealed the following key findings.

A difference between the platforms was observed depending on the number of satellites and the visibility of satellites in all parameters of the satellite geometry variation. It is clear that kinematic platform is affected from the visibility of satellites and the number of satellites more than static platforms. Differences between the kinematic and static platforms according to latitude, longitude and height components were observed to be 3, 2, 4 cm in Partial Blocked parameter, 5,11,2 cm in Half Blocked parameter, 0, 7, 0 cm in Cut-0ff Elevation (30°) parameter, 35, 47, 5 cm in Least Satellite parameter.

In the tropospheric models, no difference was observed between NIELL and SBAS models between platforms. In the Saastamonien parameter, 8 and 4 cm moving receivers in the longitude and height components, respectively yielded results more negative than those of the static receiver. In clock products, no difference was observed between longitude and height components. However, the moving receiver in the latitude component was adversely affected by all product parameters of 2-3 cm relative to the static receiver.

When the effect of the Satellite System, satellite geometry, Troposphere Correction and Clock Products parameters on convergence time was examined, no change in the convergence time between the two platforms was observed in other variations except the satellite geometry parameters.

The convergence time was affected more by this situation depending on the platform speed. The values on the Cut-0ff Elevation (30°) parameters converged only on the static platform. It was observed that the Half Block parameter converged to 10 cm accuracy in 10,20,10 minutes at latitude, longitude and height components on static platform faster than kinematic platforms.

It was observed that although 13 parameters had different effects in terms of accuracy in static and kinematic platforms the platform difference did not have an effect on the convergence time except the satellite geometry parameters. When convergence time was examined on the components, it was observed that the longitude component converges in a longer period than the other components. The longitude component can be improved significantly by resolving the integer carrier-phase ambiguities [15].It was found that observation time of 3 hours was sufficient for all parameters except GLONASS-only, LS, Saastamoinen and SBAS, IGS 5 MIN parameters. When the convergence time of the clock products is examined, unlike other parameters, the results of other clock products except code 5 seconds show that they contain noise. The use of High-rate products such as Code 5 sec as the clock product does not change the convergence time, eliminates the noise.

It is clear from all the results, including the components of latitude longitude and height, that effective parameters were more significant in the moving receiver on the kinematic platform than static receiver. Parameters such as clock products, and tropospheric correction therefore have less effect on precise positioning, especially in static platforms, than other parameters; however, their effect

increases depending on the speed of the receiver. The analysis of effective parameters on different platforms has revealed differences based on the moving or static receiver in which measurements are performed. Thus, in GNSS observations where the same parameters are applied, different results can be obtained due to different types of platforms.

AUTHORSHIP CONTRIBUTIONS

Authors equally contributed to this work.

DATA AVAILABILITY STATEMENT

The authors confirm that the data that supports the findings of this study are available within the article. Raw data that support the finding of this study are available from the corresponding author, upon reasonable request.

CONFLICT OF INTEREST

The author declared no potential conflicts of interest with respect to the research, authorship, and/or publication of this article.

ETHICS

There are no ethical issues with the publication of this manuscript.

REFERENCES

[1] Azis RA, Suhandri HF, Wijaya DD. The Study of Position Accuracy Using Precise Point Positioning (PPP) In Perspective of Indonesian National Standard of Horizontal Reference Network. E3S Web of Conferences. 2019;94:01004. [CrossRef]

[2] Chen W, Hu C, Li Z, Chen Y, Ding X, Gao S, et al. Kinematic GPS precise point positioning for sea level monitoring with GPS buoy. J Glob Position Syst 2004;3:302–307. [CrossRef]

[3] Hofmann-Wellenhof B, Lichtenegger H, Wasle E. GNSS–Global Navigation Satellite Systems: GPS, GLONASS, Galileo, and more. Wien: Springer Science & Business Media, 2017.

[4] Bisnath S, Gao Y. Current state of precise point positioning and future prospects and limitations. In Observing our changing earth. Part of the International Association of Geodesy Symposia book series: Berlin, Heidelberg, 2009:615–623. [CrossRef]

[5] Ocalan T. Accuracy assessment of gps precise point positioning (PPP) technique using different web-based online services in a forest environment. Šumarski List 2016;140:357–367. [CrossRef]

[6] Anderle RJ. (1976). Point positioning concept using precise ephemeris. In Satellite Doppler Positioning, Proceedings of the International Geodetic Symposium, Las Cruces, N. Mex., October 12-14, New Mexico: New Mexico State University, 1976;1:47–75.

[7] Zumberge JF, Heflin MB, Jefferson DC, Watkins MM, Webb FH. Precise point positioning for the efficient and robust analysis of GPS data from large networks. J Geophys Res Solid Earth 1997;102:5005–5017. [CrossRef]

[8] Kouba J, Héroux P. Precise point positioning using IGS orbit and clock products. GPS Solut 2001;5:12–28. [CrossRef]

[9] Gao Yi, Chen K. Performance analysis of precise point positioning using real-time orbit and clock products. J Glob Position Syst 2004;3:95–100. [CrossRef]

[10] Colombo OL, Sutter AW, Evans AG. Evaluation of precise, kinematic GPS point positioning. In Proceedings of ION GNSS 17th International Technical Meeting of the Satellite Division, Long Beach, California, 1423–1430, 2004.

[11] GMV (2011). PPP Standards, European Space Agency, https://gssc.esa.int/navipedia/index.php/PPP_Standards Accessed on Oct 2019.

[12] Li X, Li X, Yuan Y, Zhang K, Zhang X, Wickert J. Multi-GNSS phase delay estimation and PPP ambiguity resolution: GPS, BDS, GLONASS, Galileo. J Geodesy 2018;92:579–608. [CrossRef]

[13] Pan Z, Chai H, Kong Y. Integrating multi-GNSS to improve the performance of precise point positioning. Adv Space Res 2017;60:2596–2606. [CrossRef]

[14] Kamali O, Cocard M, Santerre R. A sequential network approach for estimating GPS satellite phase biases at the PPP-AR producer-side. GPS Solut 2018;22:59. [CrossRef]

[15] Ge M, Gendt G, Rothacher MA, Shi C, Liu J. Resolution of GPS carrier-phase ambiguities in precise point positioning (PPP) with daily observations. J Geodesy 2008;82:389–399. [CrossRef]

[16] Collins P, Lahaye F, He´rous P, Bisnath S. Precise point positioning with ambiguity resolution using the decoupled clock model. In: Proceedings of ION GNSS 2008. Institute of Navigation, Savannah, GA, 1315–1322, 2008. [CrossRef]

[17] Laurichesse D, Mercier F. Integer ambiguity resolution on undifferenced GPS phase measurements and its application to PPP. Navigation 2009;56:135–149 [CrossRef]

[18] Aggrey J, Bisnath S. Analysis of multi-GNSS PPP initialization using dual-and triple-frequency data. In Proceedings of the Proceedings of the 2017 International Technical Meeting of The Institute of Navigation, Monterey, CA, USA, 445–458, 2017. [CrossRef]

[19] Øvstedal O, Kjørsvik N, Gjevestad JG. Surveying using GPS precise point positioning. In XXII International FIG Congress, Munich, Germany, 2006.
[20] Guo F, Zhang X, Li X, Cai S. Impact of sampling rate of IGS satellite clock on precise point positioning. Geo Spat Inf Sci 2010;13:150–156. [CrossRef]
[21] Anquela AB, Martín A, Berné JL, Padín J. GPS and GLONASS static and kinematic PPP results. J Surv Eng 2012;139:47–58. [CrossRef]
[22] Dawidowicz K, Krzan G. Accuracy of single receiver static GNSS measurements under conditions of limited satellite availability. Surv Rev 2014;46:278–287. [CrossRef]
[23] De Oliveira PS, Morel L, Fund F, Legros R, Monico JFG, Durand S, et al. Modeling tropospheric wet delays with dense and sparse network configurations for PPP-RTK. GPS Solut 2017;21:237–250. [CrossRef]
[24] El-Mowafy A. Analysis of web-based GNSS post-processing services for static and kinematic positioning using short data spans. Surv Rev 2011;43:535–549. [CrossRef]
[25] Subirana JS, Zornoza JMJ, Hernández-Pajares M. Global Navigation Satellite Systems, Volume I: Fundamentals and Algorithms. ESA Communications ESTEC, Noordwijk, the Netherlands, 238, 2013.
[26] Gross JN, Watson RM, D'Urso S, Gu Y. Flight-test evaluation of kinematic precise point positioning of small UAVs. Int J Aerosp Eng 2016;22016:1259893. [CrossRef]
[27] Li X, Zhang X, Ren X, Fritsche M, Wickert J, Schuh H. Precise positioning with current multi-constellation global navigation satellite systems: GPS, GLONASS, Galileo and BeiDou. Sci Rep 2015;5:8328. [CrossRef]
[28] Misra P, Enge P. Global Positioning System: Signals, Measurements and Performance. 2nd ed. Massachusetts: Ganga-Jamuna Press, 2006. [CrossRef]
[29] Elsobeiey M, El-Rabbany A. On modelling of second-order ionospheric delay for GPS precise point positioning. J Navig 2012;65:59–72. [CrossRef]
[30] Gao Y, Chen K. Performance analysis of precise point positioning using real-time orbit and clock products. J Glob Posit Syst 2004;3:95–100. [CrossRef]
[31] Takasu T. (2013). RTKLIB ver. 2.4.2 Manual, RTKLIB: An Open Source Program Package for GNSS Positioning, pp. 154-160, Available at: http://www.rtklib.com/prog/manual_2.4.2.pdf Accessed on May 10, 2021.
[32] Weinbach U, Schön S. GNSS receiver clock modeling when using high-precision oscillators and its impact on PPP. Adv Space Res 2011;47:229–238. [CrossRef]
[33] Dabove P, Linty N, Dovis F. Analysis of multi-constellation GNSS PPP solutions under phase scintillations at high latitudes. Applied Geomatics, 2019;12:45–52. [CrossRef]
[34] Lou Y, Zheng F, Gu S, Wang C, Guo H, Feng Y. Multi-GNSS precise point positioning with raw single-frequency and dual-frequency measurement models. GPS Solut 2016;20:849–862. [CrossRef]
[35] Mendez Astudillo J, Lau L, Tang YT, Moore T. (2018). Analysing the Zenith Tropospheric Delay estimates in on-line Precise Point Positioning (PPP) services and PPP software packages. Sensors 2018;18:580.
[36] Canadian Spatial Reference System-Precise Point Positioning (CSRS-PPP) web page, Available at: https://www.nrcan.gc.ca/ Accessed on March 2021.
[37] Takasu T, Yasuda A. Development of the low-cost RTK-GPS receiver with an open source program package RTKLIB. In International symposium on GPS/GNSS (Vol. 1). International Convention Center Jeju Korea, 2009.
[38] Saastamoinen J. Atmospheric correction for the troposphere and stratosphere in radio ranging satellites. The use of artificial satellites for geodesy 1972;15:247–251. [CrossRef]
[39] Swinbank R, O'Neill A. A stratosphere-troposphere data assimilation system. Mon Weather Rev 1994;122:686–702. [CrossRef]
[40] RTCA-MOPS (1999). Minimum operational standards for global positioning system/wide area augmentation system airborne equipment. 6, Oct 1999, RTCA/DO-229 B. RTCA Inc., Washington, USA.
[41] Selbesoglu, O, Gurturk M, Soycan M. Accuracy Assessment of the Precise Point Positioning for Different Troposphere Models. In EGU General Assembly Conference, Vienna, Austria, 2016.
[42] Soycan M. A quality evaluation of precise point positioning within the Bernese GPS Software Version 5.0. Arabian. J Sci Eng 2012;37:147–162. [CrossRef]